Inorg. Chem. **2008**, *47*, 5963−5970

(α-Diimine)chromium Complexes: Molecular and Electronic Structures; A Combined Experimental and Density Functional Theoretical Study

Meenakshi Ghosh, Stephen Sproules, Thomas Weyhermüller, and Karl Wieghardt*

Max-Planck-Institut für Bioanorganische Chemie, Stiftstrasse 34-36, D-45470 Mülheim an der Ruhr, Germany

Received February 14, 2008

Dark brown crystals of $[Cr(^1L)_2]$ (**1**) were obtained from the reaction of $[Cr^{III}(acac)_3]$ ($acac^- = 2,4$-pentanedionate) with 2 equiv of 2-methyl-1,4-bis(2,6-dimethylphenyl)-1,4-diaza-1,3-butadiene (^1L) and 3 equiv of sodium in tetrahydrofuran (thf) under an Ar atmosphere. Complex **1** possesses an $S = 1$ ground state, which is attained via intramolecular antiferromagnetic coupling between a high-spin Cr^{II} ion ($S_{Cr} = 2$) and two anionic α-diiminato(1-) ligand π radicals $(^1L^{\bullet})^{1-}$. The molecular structure of **1** exhibits a distorted tetrahedral, nearly square-planar geometry. The average $C-N_{imine}$ bond length at 1.346 Å is characteristic for the π radical anion $(^1L^{\bullet})^{1-}$, and therefore, the electronic structure of **1** is best described as $[Cr^{II}(^1L^{\bullet})_2]$. This has been confirmed by broken symmetry density functional theoretical calculations BS(4,2) (DFT) at the B3LYP level. The reaction of $[Cr^{III}(acac)_3]$ with 1 equiv of 2,3-dimethyl-1,4-bis(2,6-diisopropylphenyl)-1,4-diaza-1,3-butadiene (^2L) and 1 equiv of Na in thf under Ar yields red-brown crystals of $[Cr^{III}(^2L^{\bullet})(acac)_2]$ (**2**) ($S = 1$). The oxidation of **2** with 1 equiv of $Fc(PF_6)$ (Fc^+ = ferrocenium) in CH_2Cl_2 affords crystals of $[Cr^{III}(^2L^{ox})(acac)_2](PF_6)$ (**3**) ($S = {}^3/_2$). The crystal structure determinations of **2** and **3** revealed that **2** contains a neutral, octahedral Cr^{III} species $[Cr^{III}(^2L^{\bullet})(acac)_2]$, whereas in **3** the ligand is oxidized, yielding an octahedral monocation $[Cr^{III}(^2L^{ox})(acac)_2]^+$. These electronic structures have been confirmed by DFT calculations.

Introduction

Careful structural, spectroscopic characterizations and density functional theoretical (DFT) calculations of main group element compounds containing α-diimine-type ligands have unequivocally shown that this type of ligand belongs to the growing group of redox noninnocent ligands.[1–14] Three oxidation levels have been identified, namely, the neutral α-diimines L^{ox}, their π radical monoanions $(L^{\bullet})^{1-}$, and the two-electron reduced enediamide form $(L^{Red})^{2-}$. It has been established by Raston et al.[7] and van Koten et al.,[8] in a series of complexes containing Li^+ and Zn^{2+} ions, that the $C-N_{imine}$ bond distances vary in a characteristic fashion on going from L^{ox} via $(L^{\bullet})^{1-}$ to $(L^{Red})^{2-}$. This is schematically shown in Chart 1. These experimental results have recently been nicely reproduced by DFT calculations.[13–15]

It is therefore rather surprising that tetrahedral bis(α-diimine)metal complexes of transition metal ions (M = Ni, Fe) have in the past in the organometallic literature always

* To whom correspondence should be addressed. Phone: ++49-208-306 3609. Fax: ++49-208-306 3952. E-mail: wieghardt@mpi-muelheim.mpg.de.

(1) van Koten, G.; Vrieze, K. *Adv. Organomet. Chem.* **1982**, *21*, 151.
(2) Richter, S.; Daul, C.; von Zelewsky, A. *Inorg. Chem.* **1976**, *15*, 943.
(3) Corvaja, C.; Pasimeni, L. *Chem. Phys. Lett.* **1976**, 261.
(4) Cloke, F. G. N.; Hanson, G. R.; Henderson, M. J.; Hitchcock, P. B.; Raston, C. L. *J. Chem. Soc., Chem. Commun.* **1989**, 1002.
(5) Cloke, F. G. N.; Dalby, C. I.; Henderson, M. J.; Hitchcock, P. B.; Kennard, C. H. L.; Lamb, R. N.; Raston, C. L. *J. Chem. Soc., Chem. Commun.* **1990**, 1394.
(6) Thiele, K.-H.; Lorenz, V.; Thiele, G.; Zönnchen, P.; Scholz, J. *Angew. Chem., Int. Ed. Engl.* **1994**, *33*, 1372.
(7) Gardiner, M. G.; Hanson, G. R.; Henderson, M. J.; Lee, F. C.; Raston, C. L. *Inorg. Chem.* **1994**, *33*, 2456.
(8) Rijnberg, E.; Richter, B.; Thiele, K.-H.; Boersma, J.; Veldman, N.; Spek, A. L.; van Koten, G. *Inorg. Chem.* **1998**, *37*, 56.
(9) Pott, T.; Jutzi, P.; Neumann, B.; Stammler, H.-G. *Organometallics* **2001**, *20*, 1965.
(10) Baker, R. J.; Farley, R. D.; Jones, C.; Mills, D. P.; Kloth, M.; Murphy, D. M. *Chem.—Eur. J.* **2005**, *11*, 2972.
(11) Pott, T.; Jutzi, P.; Kaim, W.; Schoeller, W. W.; Neumann, B.; Stammler, A.; Stammler, H.-G.; Wanner, M. *Organometallics* **2002**, *21*, 3169.
(12) (a) Baker, R. J.; Farley, R. D.; Jones, C.; Kloth, M.; Murphy, D. M. *Chem. Commun.* **2002**, 1196. (b) Baker, R. J.; Farley, R. D.; Jones, C.; Kloth, M.; Murphy, D. M. *Dalton Trans.* **2002**, 3844.
(13) Tuononen, H. M.; Armstrong, A. F. *Dalton Trans.* **2006**, 1885.
(14) Tuononen, H. M.; Armstrong, A. F. *Inorg. Chem.* **2005**, *44*, 8277.
(15) Muresan, N.; Chlopek, K.; Weyhermüller, T.; Neese, F.; Wieghardt, K. *Inorg. Chem.* **2007**, *46*, 5327.

10.1021/ic800290s CCC: $40.75
Published on Web 05/28/2008

Chart 1

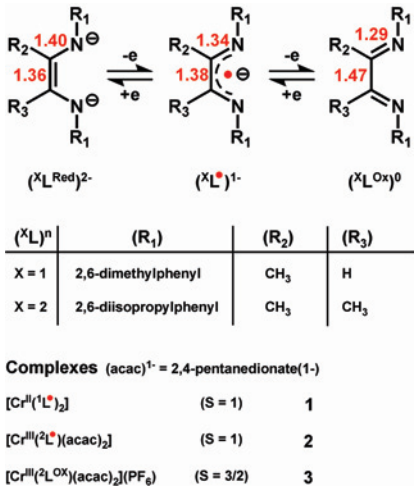

been described as $[M^0(L^{ox})_2]$ despite the fact that the corresponding *paramagnetic* zinc complex has unambiguously been identified as $[Zn^{II}(L^{\bullet})_2]$.[7,8] Only recently, it has been established that the electronic structures are correctly designated as $[Ni^{II}(L^{\bullet})_2]^0$,[15–17] and $[Fe^{II}(L^{\bullet})_2]^0$,[18] where high-spin ions Ni^{II} ($S_{Ni} = 1$) and Fe^{II} ($S_{Fe} = 2$) are intramolecularly antiferromagnetically coupled to two ligand π radical anions $(L^{\bullet})^{1-}$ ($S_{rad} = {}^1/_2$), yielding the observed singlet for the nickel and the triplet ground state for the iron complexes.

Interestingly, tom Dieck and Kinzel[19] reported in 1979 the synthesis of a similar bis(α-diimine)chromium complex, to which they assigned an electronic structure of $[Cr^0(L^{ox})_2]$, where L^{ox} represents N,N′-ethanediylidene-bis(2,4-dimethyl-3-pentaneamine) (eq 1). This complex was shown to dimerize isoprene catalytically in the presence of Et_2AlOEt.

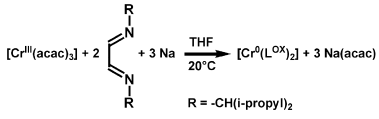

(1)

At that time, only the electronic spectrum and its mass spectrum were reported; the spin ground state of this molecule is unknown.

More recently, Theopold et al.[20] reported the synthesis and crystal structure of a planar, dinuclear species, eq 2:

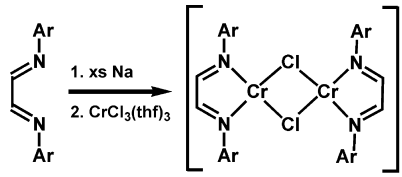

(2)

The structural formula in eq 2 appears to invoke two antiferromagnetically coupled Cr^I ions (d^5, $S = {}^3/_2$) in a square-planar environment. In contrast, the reported $C-N_{imine}$ distance at 1.340 Å and the corresponding average C−C distance within the two five-membered chelate rings at 1.388 Å point to the presence of two ligand π radicals $(L^{\bullet})^{1-}$. Therefore, we suggest that this species has an electronic structure, as in $[(L^{\bullet})Cr^{II}(\mu\text{-}Cl)_2Cr^{II}(L^{\bullet})_2]^0$, where the high-spin Cr^{II} ions (d^4, $S_{Cr} = 2$) are strongly antiferromagnetically coupled to a ligand radical ($S^* = {}^3/_2$), two of which couple to yield the observed diamagnetic ground state.

In order to shed more light on the electronic structures of coordination complexes of chromium-containing α-diimine-type ligands, we have synthesized complexes **1**, **2**, and **3**, shown in Chart 1; determined their crystal structures; and now report their magnetochemistry and electronic spectra. We will show that it is unambiguously possible to determine the oxidation state (level) of the central chromium ion and the ligands. These experimental results have been supported by broken symmetry (BS) DFT calculations by using the B3LYP functional.

Experimental Section

All air-sensitive materials were manipulated by using standard Schlenk line techniques or a glovebox. $[Cr^{III}(acac)_3]$, where $(acac)^{1-}$ represents the 2,4-pentanedionate(1-) anion, and ferrocenium hexafluorophosphate were purchased from Aldrich. The ligands 2-methyl-1,4-bis(2,6-dimethylphenyl)-1,4-diaza-1,3-butadiene, $(^1L^{ox})^0$, and 2,3-dimethyl-1,4-bis(2,6-diisopropylphenyl)-1,4-diaza-1,3-butadiene, $(^2L^{ox})$, were synthesized according to published procedures.[21]

$[Cr^{II}(^1L^{\bullet})_2]$ (1). To a solution of the ligand ($^1L^{ox}$; 0.56 g, 2.0 mmol) in dry tetrahydrofuran (thf; 20 mL) under an argon blanketing atmosphere was added sodium (0.07 g, 3.0 mmol) with stirring at 20 °C. After 20 min, $[Cr^{III}(acac)_3]$ (0.35 g, 1.0 mmol) was added to the solution, whereupon the red color of the solution turned dark brown. After being stirred for 24 h at 20 °C, the solvent was removed by evaporation under reduced pressure. The dry residue was extracted with *n*-hexane and filtered through celite. Upon partial removal of the solvent under reduced pressure, dark-brown crystals of **1** were obtained at −20 °C. Yield: 0.51 g (84%). Anal. calcd for $C_{38}H_{44}N_4Cr$: C, 75.0; H, 7.3; N, 9.2; Cr, 8.6. Found: C, 75.1; H, 7.4; N, 9.1; Cr, 8.6.

$[Cr^{III}(^2L^{\bullet})(acac)_2]^0$ (2). To a solution of the ligand ($^2L^{ox}$) (0.81 g, 2.0 mmol) in tetrahydrofuran (20 mL) under an Ar blanketing atmosphere was added sodium (0.05 g, 2.0 mmol) and $[Cr^{III}(acac)_3]^0$ (0.70 g, 2.0 mmol) with stirring at 20 °C for ∼20 h. After removal of the solvent by evaporation under reduced pressure, the dry residue was extracted with *n*-hexane and filtered through celite. X-ray-quality crystals were obtained from a concentrated *n*-hexane solution at −20 °C. Yield: 1.05 g (80%). Anal. calcd for $C_{38}H_{54}N_2O_4Cr$: C, 69.7; H, 8.3; N, 4.3; Cr, 7.9. Found: C, 69.8; H, 8.4; N, 4.2; Cr, 7.9.

$[Cr^{III}(^2L^{ox})(acac)_2](PF_6)\cdot$thf (3). To a solution of **2** (0.26 g, 0.40 mmol) in CH_2Cl_2 (10 mL) was added 1 equiv of ferrocenium

(16) Muresan, N.; Weyhermüller, T.; Wieghardt, K. *Dalton Trans.* **2007**, 4390.
(17) Khusniyarov, M. M.; Harms, K.; Burhaus, O.; Sundermeyer, J. *Eur. J. Inorg. Chem.* **2006**, 2985.
(18) Muresan, N.; Lu, C. C.; Ghosh, M.; Henling, L. E.; Peters, J.; Weyhermüller, T.; Bill, E.; Wieghardt, K. *Inorg. Chem.* In print.
(19) tom Dieck, H.; Kinzel, A. *Angew. Chem., Int. Ed. Engl.* **1979**, *18*, 324.
(20) Kreisel, K. A.; Yap, G. P. A.; Dmitrenko, O.; Landis, C. R.; Theopold, K. H. *J. Am. Chem. Soc.* **2007**, *129*, 14162.
(21) Druzhkov, N. O.; Teplova, I. A.; Glushakova, V. V.; Skorodumova, V. A.; Abakumov, G. A.; Zhao, B.; Berluche, E.; Schulz, D. N.; Baugh, L. S.; Ballinger, C. A.; Squire, K. R.; Canich, J.-A. M.; Bubnov, M. P. Patent PCT/VS 2003/022356, WO2004/007509, 2004.
(22) *ShelXTL*, v.5; Siemens Analytical X-Ray Instruments, Inc.:, Madison, WI, 1994.
(23) Sheldrick, G. M. *ShelXL97*; Universität Göttingen: Germany, 1997.

Table 1. Crystallographic Data for **1**, **2**, and **3**·thf

	1	**2**	**3**·thf
chem. formula	$C_{38}H_{44}CrN_4$	$C_{38}H_{54}CrN_2O_4$	$C_{42}H_{62}CrF_6N_2O_5P$
fw	608.77	654.83	871.91
space group	*C*2/*c*, No. 15	*C*2/*c*, No. 15	$P2_1/n$, No. 14
a, Å	10.7469(6)	21.835(2)	17.2368(3)
b, Å	13.0959(6)	12.5567(10)	12.4547(2)
c, Å	23.2424(12)	27.350(2)	20.9158(4)
β, deg	99.348(3)	90.743(7)	90.085(3)
V, Å	3227.7(3)	7498.1(11)	4490.2(2)
Z	4	8	4
T, K	100(2)	100(2)	100(2)
ρ calcd, g cm^{-3}	1.253	1.160	1.290
reflns collected/$2\Theta_{max}$	19891/66.48	55245/55.00	110846/65.00
unique reflns/$I > 2\sigma(I)$	6084/4758	8549/6022	16062/13116
no. of params/restr.	205/0	420/0	561/31
λ, Å/*μ*(Kα), cm^{-1}	0.71073/3.87	0.71073/3.44	0.71073/3.58
R1[a]/goodness of fit[b]	0.0487/ 1.041	0.0562/1.022	0.0460/ 1.030
wR2[c] ($I > 2\sigma$ (I))	0.1209	0.0950	0.1178
residual density, *e*Å^{-3}	+0.30/−0.60	+0.30/−0.46	+0.71/−0.71

[a] Observation criterion: $I > 2\sigma(I)$. $R1 = \sum||F_o| - |F_c||/\sum|F_o|$. [b] $GOF = [\sum[w(F_o^2 - F_c^2)^2]/(n - p)]^{1/2}$. [c] $wR2 = [\sum[w(F_o^2 - F_c^2)^2]/\sum[w(F_o^2)^2]]^{1/2}$, where $w = 1/\sigma^2(F_o^2) + (aP)^2 + bP$, $P = (F_o^2 + 2F_c^2)/3$.

hexafluorophosphate (0.13 g, 0.40 mmol) with stirring for 1.5 h at 20 °C. The original dark-brown color of the solution changed to green-brown. The resulting solution was filtered and the solvent removed by evaporation under reduced pressure. The residue was washed 3−4 times with *n*-hexane in order to remove ferrocene. The crude compound was dissolved in tetrahydrofuran and filtered through celite. After slow evaporation of the solvent, single crystals of X-ray quality were obtained. Yield: 0.48 g (92%). ESI mass spectrometry (pos. ion; CH_2Cl_2): *m*/*z* 654 {**3**-PF_6}$^+$. Anal. calcd for $C_{42}H_{62}N_2O_5F_6PCr$: C, 57.8; H, 7.1; N, 3.2; Cr, 6.0. Found: C, 57.9; H, 7.2; N, 3.2; Cr, 6.1.

Calculations. All calculations were performed by using the ORCA program package.[24] The geometry optimizations were carried out at the BP86 level[25a,b] of DFT. The all-electron Gaussian basis sets were those reported by the Ahlrichs group.[26,27] Triple-ζ-quality basis sets with one set of polarization functions on the chromium, oxygen, and nitrogen were used (TZVP). The carbon and hydrogen atoms were described by slightly smaller polarized split-valence SV(P) basis sets that are double-ζ-quality in the valence region and contain a polarizing set of d functions on the non-hydrogen atoms.[26] The auxiliary basis sets for all complexes used to expand the electron density in the calculations were chosen to match the orbital basis. Electronic energies and properties were calculated at the optimized geometries with the B3LYP functional.[25c,d] In this case, the same basis sets were used. The self-consistent field calculations were tightly converged (1×10^{-8} Eh in energy, 1×10^{-7} Eh in the density change, and 1×10^{-7} in the maximum element of the DIIS[25e,f] error vector). The geometry search for all complexes was carried out in redundant internal coordinates without imposing geometry constraints. Corresponding orbitals[28] and density plots were obtained by the program Molekel.[29] We describe our computational results for **1** and **2** containing noninnocent ligands using the BS approach.[30−32]

Since, for complexes **1** and **2** studied here, one can obtain broken-symmetry solutions to the spin-unrestricted Kohn−Sham equations,[30−32] we will adopt the following notation: The system is divided into two fragments. The notation BS(*m*,*n*) refers to a broken symmetry state with *m* unpaired spin-up electrons on fragment 1 and *n* unpaired spin-down electrons essentially localized on fragment 2. In most cases, fragments 1 and 2 correspond to the metal and the ligand, respectively. Note that in this notation a standard high-spin open-shell solution would be written down as BS($m+n$,0). In general, the BS(*m*,*n*) notation refers to the initial guess to the wave function. The variational process does, however, have the freedom to converge to a solution of the form BS($m-n$,0), where effectively the *n*-spin-down electrons pair with $n < m$ spin-up electrons on the partner fragment. Such a solution is then a standard $M_S = (m - n)/2$ unrestricted Kohn−Sham solution. As explained elsewhere,[28] the nature of the solution is investigated via the corresponding orbital transformation, which via the corresponding overlaps displays whether the system is to be described as a spin-coupled or a closed-shell solution.

X-Ray Crystallographic Data Collection and Refinement of the Structures. A black single crystal of **1** and orange-brown crystals of **2** and **3**·thf were coated with perfluoropolyether, picked up with nylon loops, and mounted in the nitrogen cold stream of the diffractometer. A Bruker-Nonius KappaCCD diffractometer equipped with a Mo-target rotating-anode X-ray source and a graphite monochromator (Mo Kα, $\lambda = 0.71073$ Å) was used throughout. Final cell constants were obtained from least-squares fits of all measured reflections. Intensity data were corrected for absorption using intensities of redundant reflections. The structures were readily solved by Patterson methods and subsequent difference Fourier techniques. The Bruker ShelXTL[22] software package was used for the solution, refinement, and artwork rendering of the structures. All non-hydrogen atoms were anisotropically refined, and hydrogen atoms were placed at

(24) Neese, F. *ORCA*, version 2.6, revision 4; Max Planck Institute for Bioinorganic Chemistry: Mülheim, Germany, 2007.
(25) (a) Becke, A. D. *J. Chem. Phys.* **1988**, *84*, 4524. (b) Perdew, J. P. *Phys. Rev. B* **1986**, *33*, 8822. (c) Lee, C.; Yang, W.; Parr, R. G. *Phys. Rev. B: Condens. Matter Mater. Phys.* **1988**, *37*, 785. (d) Becke, A. D. *J. Chem. Phys.* **1993**, *98*, 5648. (e) Pulay, P. *Chem. Phys. Lett.* **1980**, *73*, 393. (f) Pulay, P. *J. Comput. Chem.* **1992**, *3*, 556.
(26) Schäfer, A.; Horn, H.; Ahlrichs, R. *J. Chem. Phys.* **1992**, *97*, 2571.
(27) Schäfer, A.; Huber, C.; Ahlrichs, R. *J. Chem. Phys.* **1994**, *100*, 5829.
(28) Neese, F. *J. Phys. Chem. Solids* **2004**, *65*, 781.
(29) *Molekel I, Advances Interactive 3-Graphics for Molecular Sciences*. http://www.cscs.ch/molekel/ (accessed Apr 2008).
(30) Noodleman, L.; Peng, C. Y.; Case, D. A.; Monesca, J. M. *Coord. Chem. Rev.* **1995**, *144*, 199.
(31) (a) Noodleman, L.; Case, D. A.; Aizman, A. *J. Am. Chem. Soc.* **1988**, *110*, 1001. (b) Noodleman, L.; Davidson, E. R. *Chem. Phys.* **1986**, *109*, 131. (c) Noodleman, L.; Norman, J. G.; Osborne, J. H.; Aizman, C.; Case, D. A. *J. Am. Chem. Soc.* **1985**, *107*, 3418. (d) Noodleman, L. *J. Chem. Phys.* **1981**, *74*, 5737.
(32) Kapre, R. R.; Bothe, E.; Weyhermüller, T.; De Beer George, S.; Muresan, N.; Wieghardt, K. *Inorg. Chem.* **2007**, *46*, 7827.

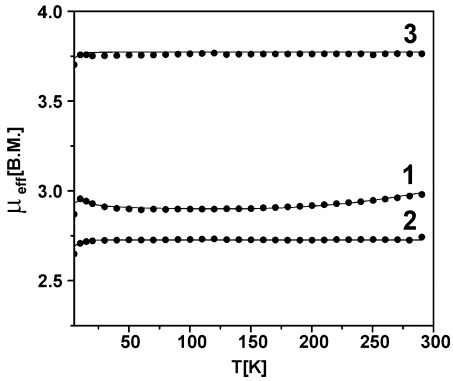

Figure 1. Temperature dependence of the magnetic moment, μ_{eff}, μ_B, of complexes **1**, **2**, and **3**. The black circles represent experimental data, whereas the solid lines represent simulations (see text).

calculated positions and refined as riding atoms with isotropic displacement parameters. Crystallographic data of the compounds are listed in Table 1.

A methyl group (C17) in complex **1** was found to be disordered over two sites. The split atom model with restrained thermal displacement parameters (EADP) yielded occupation factors of about 0.5 for each carbon position.

The thf solvent molecule in compound **3**·thf was found to be severely disordered. A split atom model with three positions was refined, giving occupation factors of about 0.63, 0.23, and 0.14. Equal thermal displacement parameters were used using the EADP instruction, and the SAME instruction of ShelXL97[23] was used to restrain C−C and C−O bond distances of thf.

Magnetic Measurements. Magnetic susceptibility data were measured from powder samples of solid material in the temperature range 2−300 K by using a SQUID susceptometer (MPMS-7, Quantum Design) with a field of 1.0 T. The experimental data were corrected for underlying diamagnetism by the use of tabulated Pascal's constants, as well as for temperature-independent paramagnetism. The susceptibility and magnetization data were simulated with our own package julX for exchange coupled systems written by Dr. E. Bill Powder summations were done by using a 16-point Lebedev grid. Intermolecular interactions were considered by using a Weiss temperature, Θ_W, as perturbation of the temperature scale, $kT' = k(T - \Theta_W)$ for the calculation.

Results

a. Syntheses and Characterization. The reaction of $[Cr^{III}(acac)_3]$ with 2 equiv of the ligand ($^1L^{ox}$; Chart 1) in thf at 20 °C affords, upon the addition of 3 equiv of sodium under strictly anaerobic conditions, dark brown crystals of $[Cr(^1L)_2]$ (**1**). Note that the generic notation (^xL) denotes a given α-diimine ligand irrespective of its oxidation level which can be specified as neutral α-diimine $(^xL^{ox})^0$ or its reduced π radical anion $(^xL^{\bullet})^{1-}$, or its doubly reduced enediamide dianion $(^xL^{Red})^{2-}$. The above synthetic procedure, shown in eq 3, follows the recipe described by tom Dieck and Kinzel[19] for $[Cr(L)_2]$, where L represents the ligand N,N′-ethanediyliden-bis(2,4-dimethyl-3-pentaneamine).

$$[Cr^{III}(acac)_3] + 2(^1L^{ox}) + 3Na \xrightarrow[20\,^\circ C]{thf} [Cr(^1L)_2]^0 + 3Na(acac) \quad (3)$$

From the temperature-dependent magnetic susceptibility measurements of a powder sample of **1** (1.0 T), it follows

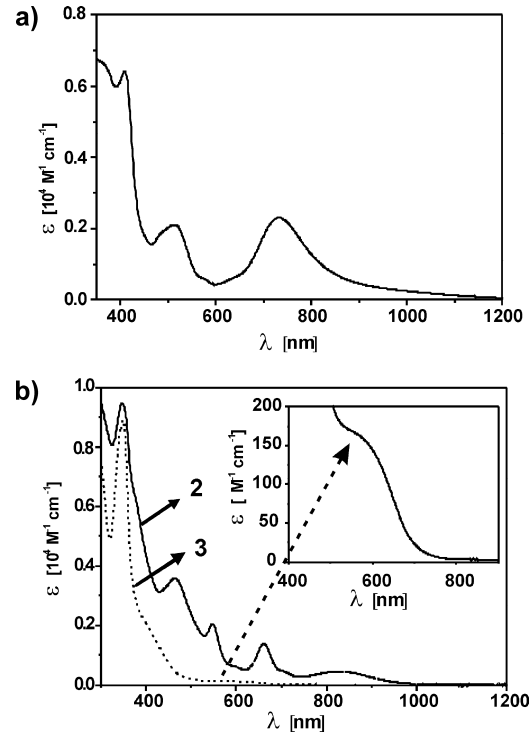

Figure 2. (a) Electronic spectrum of **1** in CH_2Cl_2 at 22 °C. (b) The corresponding spectra of **2** (solid line) and **3** (broken line) in CH_2Cl_2 at 22 °C. The inset shows the spectrum of **3** in the visible region.

that **1** possesses a triplet ground state ($S = 1$). The effective magnetic moment is constant at 2.90 μ_B between 30 and ~200 K but increases slightly to 3.0 μ_B at 290 K (Figure 1). This increase was tentatively modeled by assuming a central high-spin Cr^{II} ion ($S_{Cr} = 2$) coupled antiferromagnetically to two ligand π radical anions $(^1L^{\bullet})^{1-}$ ($S_{rad} = {}^1/_2$). Using the spin Hamiltonian eq 4, a coupling constant of $J = -215$ cm^{-1} was obtained together with g values of 2.02 for Cr^{II} and 2.0 for the radicals.

$$\hat{H} = -2J\left[\hat{\vec{S}}_{Cr}\cdot\hat{\vec{S}}_{rad,1} + \hat{\vec{S}}_{Cr}\cdot\hat{\vec{S}}_{rad,2}\right] + \mu_B\left[g_{Cr}\hat{\vec{S}}_{Cr} + g_{rad}\left(\hat{\vec{S}}_{rad,1} + \hat{\vec{S}}_{rad,2}\right)\right]\cdot\vec{B} + D_{Cr}\left[S^2_{Cr,z} - 2\right] \quad (4)$$

The increase at low temperatures is due to weak ferromagnetic intermolecular interaction according to a Weiss temperature $\Theta_{Weiss} = +0.7$ K. The effect was superimposed by a decrease of the magnetic moments due to zero-field splitting from the Cr^{II} ion with $|D|_{Cr} = 1.7$ (±1.5) cm^{-1}.

This model implies that the electronic structure of **1** should be described as $[Cr^{II}(^1L^{\bullet})_2]$ and not as $[Cr^0(^1L^{ox})_2]$. Figure 2a shows the electronic spectrum of **1** in CH_2Cl_2. Three intense absorption maxima at 730, 500, and 410 nm ($\varepsilon > 0.2 \times 10^4$ M^{-1} cm^{-1}) are tentatively assigned as intraligand transitions of the π radical anions.

When a solution of $[Cr(acac)_3]$ in thf was treated with 1 equiv of the ligand ($^2L^{ox}$) and 1 equiv of sodium under strictly anaerobic conditions at 20 °C, red-brown crystals of $[Cr(^2L)(acac)_2]$ (**2**) were obtained in good yields, eq 5.

$$[\mathrm{Cr(acac)_3}] + ({}^2\mathrm{L^{ox}}) + \mathrm{Na} \xrightarrow[20\,^\circ\mathrm{C}]{\mathrm{thf}} [\mathrm{Cr}({}^2\mathrm{L})(\mathrm{acac})_2] + \mathrm{Na(acac)} \quad (5)$$

As shown in Figure 1, a temperature-independent magnetic moment (5−295 K) of 2.75 μ_B indicates a triplet ground state ($S = 1$) for **2** which is attained via strong intramolecular antiferromagnetic coupling between a central Cr^{III} ion ($S_{Cr} = {}^3/_2$) and a single π radical anion $({}^2L^{\bullet})^{1-}$ ($S_{rad} = {}^1/_2$). A simulation using eq 6 yields $g_{Cr} = 1.94$ and $D_{Cr} = 2\ cm^{-1}$, with g_{rad} fixed to 2.

$$\hat{H} = -2J\hat{\vec{S}}_{Cr}\cdot\hat{\vec{S}}_{rad} + \mu_B\left(g_{Cr}\hat{\vec{S}}_{Cr} + g_{rad}\hat{\vec{S}}_{rad}\right)\vec{B} + D_{Cr}\left[S^2_{Cr,z} - 5/4\right] \quad (6)$$

The lower g value of Cr^{III}, compared to that of Cr^{II} found in **1**, is the reason that the trace of **2** is lower than that of **1**. For the Cr^{III}−radical coupling in **2**, only a lower limit can be given: $-J > 450\ cm^{-1}$ (as used for the actual result).

The electronic spectrum of **2** shown in Figure 2b displays intense ($\varepsilon > 0.1 \times 10^4\ M^{-1}\ cm^{-1}$) absorption maxima in the visible region at 680, 560, and 460 nm characteristic of the presence of a ligand π radical anion, as in **1**.

We conclude that the electronic structure of octahedral **2** should be described as $[Cr^{III}({}^2L^{\bullet})(acac)_2]^0$. Interestingly, **2** can be chemically (by ferrocenium hexafluorophosphate) or electrochemically (reversibly) one-electron oxidized, eq 7.

$$[Cr^{III}({}^2L^{\bullet})(acac)_2]^0 + [Fc]PF_6 \rightarrow [Cr^{III}({}^2L^{ox})(acac)_2](PF_6) + Fc^0 \quad (7)$$

Thus, from a CH_2Cl_2 solution of **2**, greenish-brown crystals of $[Cr^{III}({}^2L^{ox})(acac)_2](PF_6)$ (**3**) were obtained upon the addition of 1 equiv of $Fc(PF_6)$.

From temperature-dependent magnetic susceptibility measurements, it was established (Figure 1) that **3** possesses an $S = {}^3/_2$ ground state ($\mu_{eff} = 3.75\ \mu_B$, 3−295 K) as is expected for an octahedral chromium(III) (d^3) species with six closed-shell ligands.

The simulation using eq 8 yields $g_{Cr} = 1.94$, in nice agreement with the result found for **2**, whereas the zero-field parameter D_{Cr} can only be estimated as $|D|_{Cr} < 0.5\ cm^{-1}$.

$$\hat{H} = \mu_B g_{Cr}\hat{\vec{S}}_{Cr}\cdot\vec{B} + D_{Cr}\left[S^2_{Cr,z} - 5/4\right] \quad (8)$$

Its electronic spectrum lacks the intense ($\varepsilon > 10^3\ M^{-1}\ cm^{-1}$) transitions in the visible (Figure 2b), which are seen in the spectra of **1** and **2**. Instead, a weak d−d transition is observed at ∼600 nm ($\varepsilon \sim 150\ M^{-1}\ cm^{-1}$).

The above data are in accord with the notion that the cation in **3** has an electronic structure which is best described as $[Cr^{III}({}^2L^{ox})(acac)_2]^+$. Thus, the one-electron oxidation of **2** affording **3** is ligand-based.

b. Electrochemistry. Figure 3 exhibits the cyclic voltammograms (CVs) of **1** and **2** in CH_2Cl_2 (0.10 M $[N(n\text{-}Bu)_4]PF_6$ supporting electrolyte) recorded at 22 °C.

The CV of **1** displays two reversible one-electron transfer waves at $E_{1/2}{}^1 = -0.39$ V and $E_{1/2}{}^2 = -0.78$ V and, in addition, an irreversible reduction peak at −1.9 V which was not studied in further detail. Both reversible waves involve oxidations of **1**, yielding a monocation and a dication, eq 9.

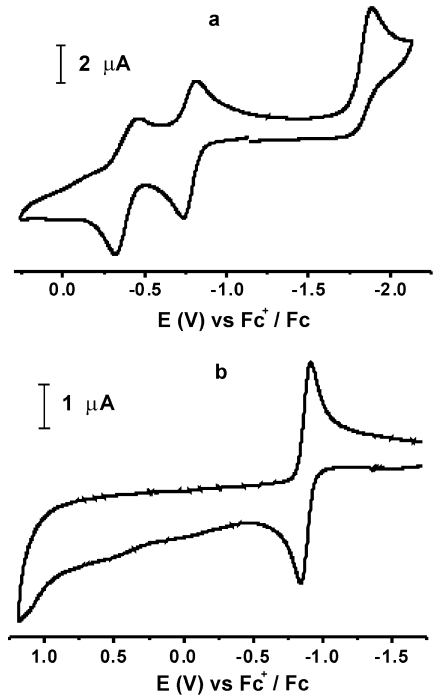

Figure 3. Cyclic voltammograms of **1** (top) and **2** (bottom) in CH_2Cl_2 at 22 °C. Conditions: 0.10 M $[N(n\text{-}Bu)_4]PF_6$ supporting electrolyte; scan rate, 100 mV s^{-1}; glassy carbon working electrode.

$$[Cr^{II}({}^1L^{\bullet})_2]^0 \underset{-e}{\overset{+e}{\rightleftharpoons}} [Cr^{I}({}^1L^{ox})({}^1L^{\bullet})]^+ \underset{-e}{\overset{+e}{\rightleftharpoons}} [Cr^{II}({}^1L^{ox})_2]^{2+} \quad (9)$$
$$E^2_{1/2} \qquad E^1_{1/2}$$

We propose that both processes are essentially ligand-based where the coordinated π radical anions $({}^1L^{\bullet})^{1-}$ are successively oxidized to the neutral α-diimines $({}^1L^{ox})^0$. Very similar CVs have been reported for $[Ni^{II}(L^{\bullet})_2]$ species,[15,16] where values for $E_{1/2}{}^1$ of ∼−0.2 V and $E_{1/2}{}^2$ of ∼−0.70 V have been reported. The monocation $[Ni(L)_2]^+$ has been shown by X-ray crystallography to contain two neutral (L^{ox}) ligands and a Ni(I) center. Here, we prefer an electronic structure for the monocation as in $[Cr^{II}({}^1L^{ox})({}^1L^{\bullet})]^+$, but with the data at hand, this remains speculative.

The CV of **2** displays a single, reversible one-electron transfer wave at $E_{1/2} = -0.80$ V versus Fc^+/Fc according to eq 10.

$$[Cr^{III}({}^1L^{\bullet})(acac)_2]^0 \underset{-e}{\overset{+e}{\rightleftharpoons}} [Cr^{III}({}^1L^{ox})(acac)_2]^+ \quad (10)$$
$$E_{1/2}$$

c. X-Ray Structures. The structures of **1**, **2**, and **3** have been determined by single-crystal X-ray crystallography at 100(2) K. Table 1 summarizes crystallographic data, and Table 2 summarizes important bond lengths and angles. Figure 4 shows the structure of a neutral molecule in crystals of **1**, and Figure 5 shows that of a molecule in crystals of **2**; Figure 6 displays the structure of a monocation in **3**.

The neutral complex $[Cr^{II}({}^1L^{\bullet})_2]$ contains two N,N′-coordinated π radical anions $({}^1L^{\bullet})^{1-}$ as is clearly established

Table 2. Selected Experimental and Calculated Bond Distances [Å] in **1**, **2**, and **3**

	1			2		3	
	exp.	calcd		exp.	calcd	exp.	calcd
Cr1−N1	2.019(1)	2.053	Cr1−N1	1.995(2)	2.023	2.099(1)	2.112
Cr1−N4	2.030(1)	2.041	Cr1−N4	2.014(2)	2.005	2.109(1)	2.112
N1−C2	1.351(2)	1.356	Cr1−O31	1.981(1)	1.989	1.939(1)	1.952
N4−C3	1.344(2)	1.367	Cr1−O35	1.987(2)	1.998	1.953(1)	1.969
C2−C3	1.395(2)	1.406	Cr1−O41	2.006(1)	2.006	1.938(1)	1.952
N1−C11	1.428(2)	1.428	Cr1−O45	2.006(2)	2.009	1.948(1)	1.969
N4−C5	1.428(2)	1.433	N1−C2	1.353(3)	1.356	1.289(2)	1.308
			N4−C3	1.357(3)	1.357	1.290(2)	1.308
			C2−C3	1.420(2)	1.424	1.512(2)	1.495
			N1−C11	1.445(3)	1.435	1.451(2)	1.441
			N4−C5	1.442(3)	1.433	1.456(2)	1.441

by the average C−N bond length at 1.348 Å (see Chart 1); the C−C bond distance in the five-membered chelate ring at 1.395 Å is also in excellent agreement with this notion. These parameters exclude formulations as $[Cr^0(^1L^{ox})_2]$ or $[Cr^{IV}(^1L^{red})_2]$; they render the physical oxidation state of the central chromium as +II (d^4; high-spin).

It is interesting that the CrN_4 coordination polyhedron in **1** is nearly *square-planar* since the dihedral angle θ between the two Cr−N−C−C−N five-membered chelate rings is 23.7° (in a perfectly square-planar arrangement, $\theta = 0$, and in a tetrahedral one, $\theta = 90°$). This dihedral angle is 48° in the corresponding complex $[Ni^{II}(^2L^{\bullet})_2]$.[15,16]

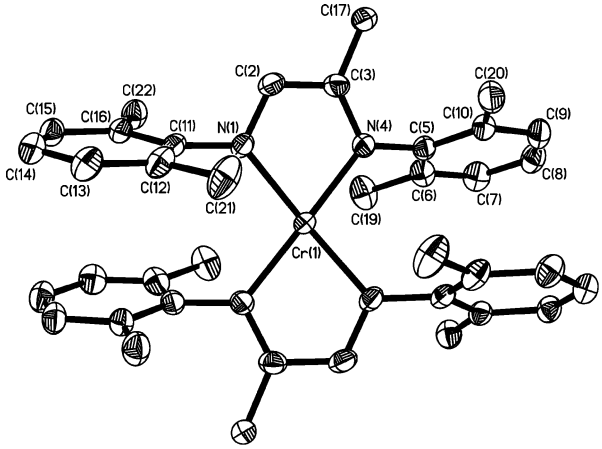

Figure 4. Structure of a neutral molecule in crystals of **1**.

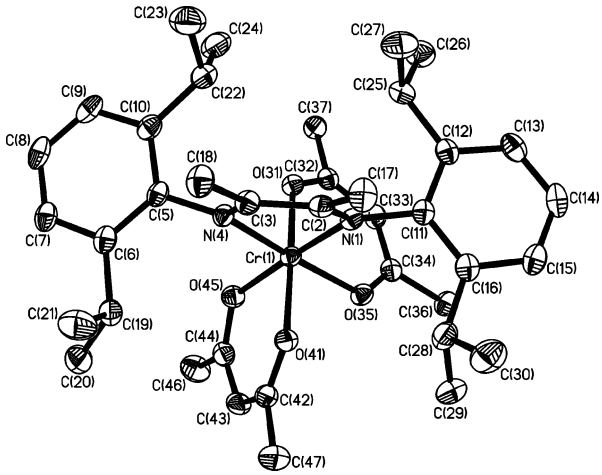

Figure 5. Structure of a neutral molecule in crystals of **2**.

It is now immediately evident that $[Cr^{II}(^1L^{\bullet})_2]$ should exist in two geometrical isomers, namely, in a transoid and in a cisoid form (see below). Both forms cocrystallize in **1** in a 1:1 ratio; they are statically disordered, which is born out by the fact that each ligand ^1L apparently carries two methyl carbon atoms C(17) and C(17)*, each with an occupancy of 0.5. Atoms N(1), N(4), C(2), and C(3) have also been refined in two split positions (occupancy 0.5).

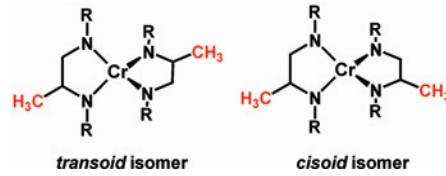

The CrN_2O_4 coordination polyhedron of neutral $[Cr^{III}(^2L^{\bullet})(acac)_2]$ (**2**) is slightly distorted octahedral (Figure 5); there are two bidentate 2,4-pentanedionate(1-) ligands and a single N,N′-coordinated π radical anion $(^2L^{\bullet})^{1-}$. The average N−C bond length at 1.355 Å and the C2−C3 bond distance at 1.420 in $(^2L^{\bullet})^{1-}$ are only compatible with a formulation as a radical anion (Chart 1). This assignment renders the oxidation state of the central chromium ion +III (d^3). The metrical details of the $Cr^{III}(acac)_2$ unit in **2** are very similar to those reported for $[Cr^{III}(acac)_3]^0$.[33]

The structure of the monocation in crystals of **3** is very similar to that of the neutral molecules in **2**. There are significant differences in the C−N and C−C distances at 1.289 and 1.512 Å, respectively, in the monocation of **3**, which are 1.355 and 1.420 Å, respectively, in neutral **2**. This is exactly the difference one would expect on going from the π radical anion $(^2L^{\bullet})^{1-}$ in **2** to the oxidized form $(^2L^{ox})$ in **3**. Thus, the redox activity of **2** and **3** is ligand-based.

d. Calculations. A picture of the electronic structures of complexes **1**, **2**, and **3** is derived from BS DFT calculations by using the B3LYP functional for the molecular orbital (MO) descriptions and—most significantly—the spin distributions in these complexes. In general, we found that the optimized geometries of all calculated complexes agree very well with the X-ray structural data (Table 2).

The geometry of the monocation in **3** was calculated spin-unrestricted ($S = {}^3/_2$) where the isopropyl substituents were replaced with methyl groups to decrease computation time.

(33) Morosin, B. *Acta Crystallogr.* **1965**, *19*, 131.

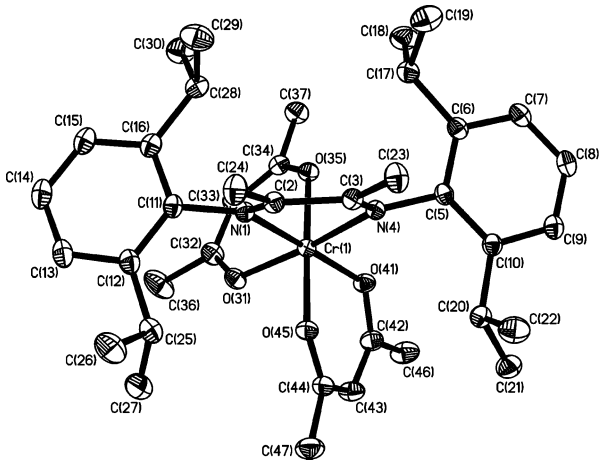

Figure 6. Structure of the monocation in crystals of **3**.

The calculated C−O, C−N, and C−C distances of the ligands are in excellent agreement with experimental results (±0.01 Å). Importantly, the calculated C−N_{imine} and C−C distances of the five-membered chelate ring imply the presence of a N,N′-coordinated ($^2L^{ox}$) ligand. In the qualitative MO bonding scheme (not shown) derived from this spin-unrestricted calculation, five orbitals of predominantly metal d character (>90%) were identified; three of these are occupied with a single electron (t_{2g}^3). This is the hallmark of a Cr^{III} (d^3) ion. The Mulliken spin density analysis displays three unpaired electrons at the Cr^{III} ion and no spin density on any of the three ligands, which are all closed-shell. These DFT calculations are in full agreement with simple ligand field theoretical considerations for an octahedral chromium(III) species.

Similarly, the geometry of the neutral species in **2** was calculated by using a BS(3,1) $M_S = 1$ state. Again, the agreement of geometrical features between the calculation and experimental results is excellent. Most importantly, the average C−N_{imine} and C−C bond distances of the five-membered chelate ring are faithfully reproduced at 1.356 and 1.424 Å, respectively, indicating the presence of a π radical anion $(^2L^{\bullet})^{1-}$ in **2**.

Figure 7 shows a qualitative MO scheme of the corresponding orbitals of magnetic pairs and metal-d orbitals of **2** and, at the bottom, a spin density plot of **2** together with approximate values of the spin density of the Mulliken spin population analysis. Five metal-d orbitals are identified, of which three are singly occupied with parallel spins (α-spin). This pattern defines again a Cr^{III} configuration at the metal center. In addition, a single ligand-centered orbital at the ^2L ligand is identified in the spin-down manifold, which is not populated in the spin-up manifold, thus leading to the observed overall $M_S = 1$ state. Complex **2** therefore features a Cr^{III} ion which is strongly antiferromagnetically coupled to a ligand π radical. The Mulliken spin density analysis confirms that there are three electrons at the Cr^{III} center (α-spin), and one unpaired electron resides in a π^* orbital of the α-diimine ligand (β-spin). No significant spin density has been identified on the two $acac^-$ ligands.

The geometry of the neutral complex in **1** was calculated by using a BS(4,2) $M_S = 1$ state. Agreement between the calculated and experimental structure (Table 2) is excellent. In particular, the average C−N_{imine} bond distance (1.362 Å (calcd) and 1.347 Å (exp)) is indicative of the presence of two π radical anions $(^2L^{\bullet})^{1-}$. It is also gratifying that the calculated dihedral angle between the two five-membered chelate rings at 37.2° is in reasonable agreement with the experimental one at 23.7°.

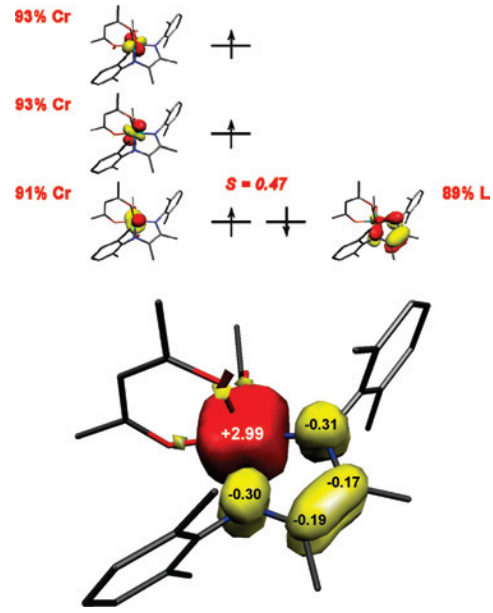

Figure 7. Top: Qualitative MO diagram for **2** of the corresponding orbitals[28] of magnetic pairs calculated at the B3LYP/TZV(P) level. Bottom: Spin density plot of **2** as derived from BS DFT calculations together with values of the spin density of the Mulliken spin population analysis.

Figure 8 exhibits a qualitative MO scheme of the spin-unrestricted corresponding orbitals of magnetic pairs and metal-d orbitals of **1**. Four singly occupied metal-d orbitals (spin-up manifold) are identified which define a high-spin chromium(II) ion. In addition, two singly occupied ligand orbitals are identified in the spin-down manifold which are not populated in the spin-up manifold; this leads to the observed overall $M_S = 1$ state. Complex **1** features a Cr^{II} ion which is strongly antiferromagnetically coupled to two ligand π radical anions: $[Cr^{II}(^1L^{\bullet})_2]$.

Figure 8 (bottom) also displays the spin density from a Mulliken spin population analysis. Four unpaired electrons (α-spin) reside on the central chromium(II) ion, and a single unpaired electron resides on each of the α-diiminate ligands $(^1L^{\bullet})^{1-}$.

Discussion

Previously, it has been shown that bis(α-diimine)metal complexes of Zn,[7,8,15] Ni,[15–17] and Fe[18] possess an electronic structure which invariably invokes a divalent central transition metal ion (Zn^{II}, Ni^{II}, and Fe^{II}) and two π radical monoanions $(L^{\bullet})^{1-}$: $[M^{II}(L^{\bullet})_2]$. The observed ground states $S = 0$ and 1 for the Zn^{II} complex, $S = 0$ for the Ni^{II}, and $S = 1$ for the Fe^{II} are composed of (a) two antiferromagnetically or ferromagnetically coupled ligand π radicals in $[Zn^{II}(L^{\bullet})_2]$ where both states are isoenergetic, (b) two π radicals which are intramolecularly antiferromagnetically coupled to a central nickel(II) ion ($S_{Ni} = 1$, d^8), or, similarly,

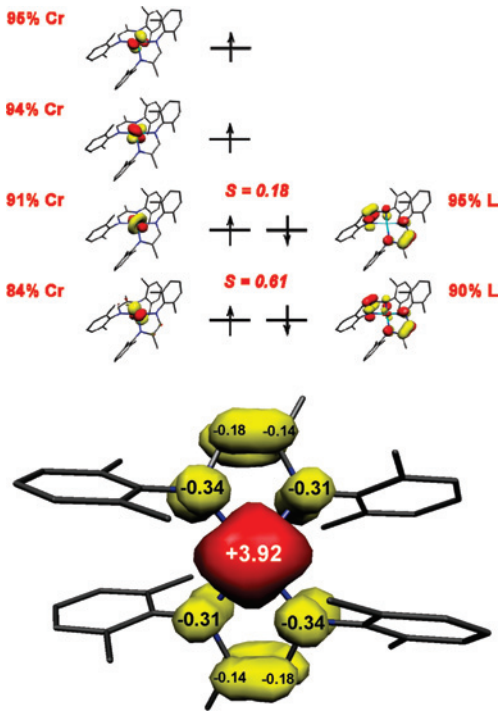

Figure 8. Top: Qualitative MO diagram for a **1** of corresponding orbitals[28] of magnetic pairs. Bottom: Spin density plot of **1** (red, α spin; yellow, β spin) together with values of the spin density of the Mulliken spin population analysis.

(c) two π radicals antiferromagnetically coupled to a central high-spin ferrous ion ($S_{Fe} = 2$, d^6). It is therefore gratifying that the same scheme holds for **1**. Clearly, two ligand π radical anions are antiferromagnetically coupled to a high-spin chromium(II) ion ($S_{Cr} = 2$, d^4): $[Cr^{II}(^1L^{\bullet})_2]$.

These results have been corroborated by the common structural features of the N,N′-coordinated $(L^{\bullet})^{1-}$ ligands where the average $C-N_{imine}$ bond distance is observed at ~1.34 Å (Chart 1) and, more convincingly, the broken symmetry calculation on each of these species including the present **1** displays a spin density of about one electron per ligand and the correct number of unpaired electrons for a given divalent first-row transition metal ion.

In all of these cases, we have not found any evidence for "low valent" complexes involving Ni(0), Fe(0), or Cr(0) as described in the previous literature. It is interesting that the octahedral complex **2** contains one $(^2L^{\bullet})^{1-}$ radical anion and a central chromium(III) ion ($S_{Cr} = {}^3/_2$) which are antiferromagnetically coupled, yielding the observed triplet ground state. Similar results have been reported for octahedral Cr^{III} complexes containing a single O,O′-coordinated *o*-benzosemiquinone.[34] It is therefore very likely that Wilkinson's complex[35] $[Cr(o\text{-}C_6H_4(NH)_2)Cl_2(PMe_2Ph)_2]$ ($S = 1$) contains an *o*-phenylenediamide(1-) π radical and does not possess a central Cr^{IV} ion (as reported) but rather is a chromium(III) species with a N,N′-coordinated π radical anion. The reported geometrical features of the radical ligand are in full agreement with this assignment.[36] As pointed out in the Introduction, Theopold et al.'s[20] dinuclear complex should be formulated as $[(L^{\bullet})Cr^{II}(\mu\text{-}Cl)_2Cr^{II}(L^{\bullet})]^0$ since the reported dimensions of the α-diimine ligand are those typical for a π radical anion.

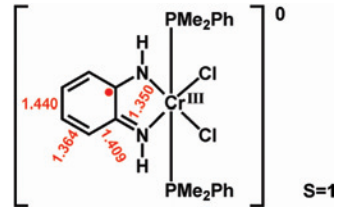

Finally, we have recently shown that α-iminopyridine ligands are also redox noninnocent. The synthesis and structural as well as spectroscopic characterization of the five-coordinate species $[Cr^{II}(\alpha\text{-iminopyridinate}^{\bullet})_2(diethyl)]$ with a triplet ground-state also contains two π radical anions.[37]

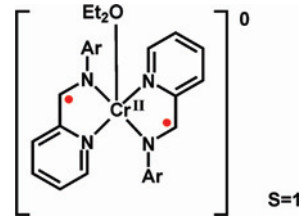

In summary, we have shown that early transition metal ions such as Cr^{II} and Cr^{III} readily form complexes with N,N′-coordinated, redox noninnocent α-diimine-type ligands. The π radical monoanion represents a quite common oxidation level in this chemistry.

Acknowledgment. We thank the Fonds of the Chemical Industry for financial support. M.G. and S.S. are grateful for a Max-Planck postdoctoral fellowship.

Supporting Information Available: X-ray crystallographic CIF files for complexes **1**, **2**, and **3**. This material is free of charge via the Internet at http://pubs.acs.org.

IC800290S

(34) (a) Wheeler, D. E.; McCusker, J. K. *Inorg. Chem.* **1998**, *37*, 2296. (b) Rodriguez, J. H.; Wheeler, D. E.; McCusker, J. K. *J. Am. Chem. Soc.* **1998**, *120*, 12051.

(35) Leung, W.-H.; Danopoulos, A. A.; Wilkinson, G.; Hussain-Bates, B.; Hursthouse, M. B. *J. Chem. Soc., Dalton Trans.* **1991**, 2051.

(36) Chlopek, K.; Bothe, E.; Neese, F.; Weyhermüller, T.; Wieghardt, K. *Inorg. Chem.* **2006**, *45*, 6298.

(37) Lu, C. C.; Bill, E.; Weyhermüller, T.; Bothe, E.; Wieghardt, K. *J. Am. Chem. Soc.* **2008**, *130*, 3181.